Desalination and Water Treatment
www.deswater.com
1944-3994/1944-3986 © 2013 Desalination Publications. All rights reserved
doi: 10.1080/19443994.2012.715076

51 (2013) 1377–1384
February

Taylor & Francis
Taylor & Francis Group

Multi-dimensional simulation tool development for the performance evaluation of a CDI electrode and its geometry parameter optimization

Byong Guk Jeon, Hee Cheon NO*

Department of Nuclear and Quantum Engineering, Korea Advanced Institute of Science and Technology, 373-1 Guseong-Dong Youseong-Gu, Daejeon 305-701, Republic of Korea
Email: hcno@kaist.ac.kr

Received 29 February 2012; Accepted 18 July 2012

ABSTRACT

A steep increase in water demand and desertification has brought about much interest in desalination. Among existing desalination methods, capacitive deionization (CDI) gets attention due to its lower cost and simpleness. The most influential factor on CDI lies on the quality of electrodes. Though various investigations and developments of electrodes have been aroused recently, no distinct standard and systematic comparison of those electrodes has been made. By solving Poisson–Nernst–Planck equations simultaneously, a simulation tool for a CDI electrode is developed. The simulation domain of the tool involves geometrical factors of electrodes, such as pore depth and pore width, in a two-dimensional manner. Using the tool, the most effective design parameters of CDI electrodes are obtained: pore depth, pore radius, capacitance, and pore diffusion coefficient. Since the capacitance and pore diffusion coefficient are not predictable in a theoretical way, those values are experimentally obtained with the support of the simulation tool. The capacitance and diffusion coefficient are calculated by our developed tool. The carbon aerogel electrode is found to have its average capacitance of 7.5 $\mu F/cm^2$ and diffusion coefficient on the order of one hundredth of bulk diffusion coefficient. Also, we found out that the diffusion coefficient at the electrode recovery phase is by 3–6 times higher than that at the salt removal phase. The diffusion coefficients increase gradually as potential decreases because of the decreased concentration of ions inside pores.

Keywords: CDI; Simulation; Electrode; Optimization

1. Introduction

In a MIT forum held in 2003, water was selected as a second problem among humanity's top 10 problems for the next 50 years. Worldwide, 2.7 billion people are suffering from water shortages and the number is expected to reach two-thirds of world population by 2025. To meet the growing demand of fresh water, increasing number of desalination plants are under construction. Among various desalination technologies, the dominant one is absolutely reverse osmosis (RO) with 61.1% world water capacity. By developing more efficient membranes and energy

*Corresponding author.

Presented at the International Conference on Desalination for the Environment, Clean Water and Energy, European Desalination Society, 23–26 April 2012, Barcelona, Spain

recovery devices, RO's cost dropped in the range 0.26–1.33 and 0.44–10 $/m^3$ for brackish water and sea water, respectively [1]. However, the cost is regarded as expensive and better desalination technologies are looked forward to. Capacitive deionization (CDI) is the right technology to save a process cost. For brackish water treatment, the cost of CDI is reported to be one third compared to that of RO [2].

The operating mechanism of CDI is simple. The CDI facility is comprised of a pair of parallel electrodes which have a small gap to allow saline water passage as shown in Fig. 1. The operation can be divided into two, a salt removal phase and an electrode recovery phase. In the salt removal phase, we apply a voltage difference (1–1.5 V) between the parallel electrodes and insert saline water in the gap of the electrodes. Salt ions in the saline water are adsorbed onto surface of pores in the electrodes. As a result, the less concentrated water, or drinkable water, is obtained at the outlet of the CDI facility. To maximize adsorption amount, we use porous carbon electrodes that have specific areas in the order of 100 m^2/g. When the capacity of electrodes reaches almost full, the electrode recovery phase starts. The CDI facility is short-circuited or is given a reverse potential, and flushing water is inserted. Since the adsorbed ions are released onto the flushing water, we can clean the electrodes and use them again. One of the strengths on CDI is this easiness in electrode recovery that avoids any complicated chemical or mechanical treatments.

Though the concept of CDI was suggested in mid-1960s, development of the technology was processed quite slowly and there exist few commercialized products in the world; one example is the Voltea company that has used CDI for cooling towers and waste water reuse. The main reason for the sluggish commercialization lies on the development of CDI electrodes. The reliable carbon aerogel electrode, that is stable under water flow, appeared in 1990s [3]. Though the electrode showed good performance, it had a problem of high price. No distinct progress on the electrode development was made until the introduction of various mesoporous carbon electrodes and activated carbon electrodes from 2000s [4–6]. The mesoporous electrodes have nominal pore sizes of several nanometers that are known to be large enough for transport and adsorption of salt ions. The activated carbon electrodes gets attention because they are cheap compared to carbon aerogel electrodes and mesoporous electrodes. The comparison of mesoporous electrodes with activated carbon electrodes for desalination purpose is not quantified as of now. To enhance the performance of CDI, aside modifying carbon electrodes themselves, adoption and coating of ion-exchange membranes in front of electrodes are also tried [7]. The membranes limit release of co-ions to enlarge the adsorption capacity of electrodes.

The process on CDI involves complex phenomena such as ion transport in a porous body, adsorption of ions, and chemical (or leakage) reactions. The understanding of mechanism on CDI is insufficient and main system parameters on the performance of CDI also need to be clarified. The first interpretation of CDI operation based on Gouy–Chapman–Stern model was made in 2010 [8]. We further expanded the

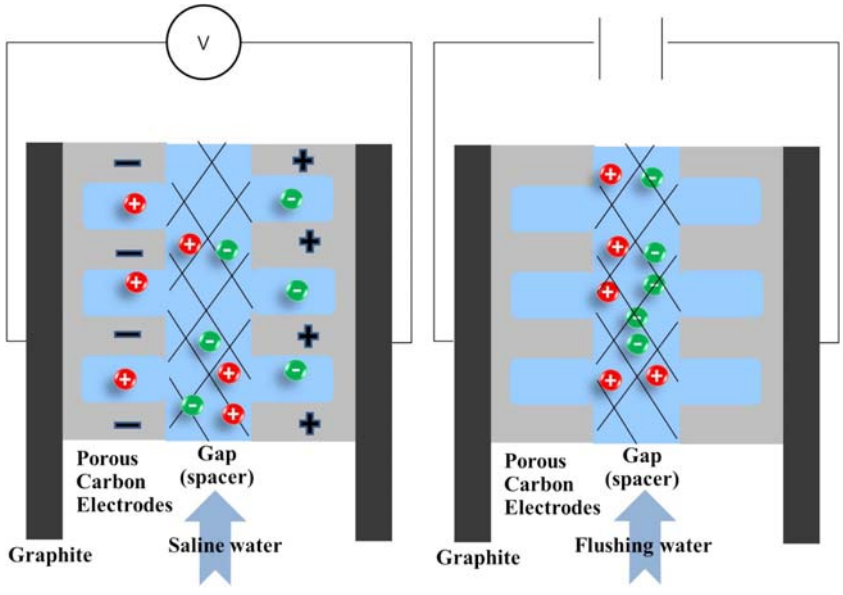

Fig. 1. Operating procedure of CDI technology (left: salt removal phase, right: electrode recovery phase).

analysis by considering geometry of CDI electrodes in a two-dimensional manner [9,10].

2. Theoretical analysis of CDI operation

To interpret operation of CDI, we should track salt ions inside a CDI facility. The most generalized model for ion transport is Poisson–Nernst–Planck (PNP) equation as shown below for NaCl solution:

Poisson's equation:

$$\nabla^2\varphi = -\frac{\rho}{\varepsilon}, \text{ where } \rho = F(C_+ - C_-), \quad (1)$$

where φ, ρ, ε, F, C_+, and C_- represent potential (V), excess charge (C/m^3), permittivity (F/m), Faraday's constant (C/mol), positive ion concentration (mol/m^3), and negative ion concentration (mol/m^3), respectively.

The Nernst–Planck equations with a convection term (written as modified NP equations):

$$\frac{\partial C_+}{\partial t} = D\nabla^2 C_+ + \frac{DF}{RT}\nabla(C_+\nabla\varphi) - U\nabla C_+, \quad (2)$$

$$\frac{\partial C_-}{\partial t} = D\nabla^2 C_- - \frac{DF}{RT}\nabla(C_-\nabla\varphi) - U\nabla C_-, \quad (3)$$

where t, D, R, T, and U represent time (s), diffusion coefficient (m^2/s), gas constant (J/mol/K), temperature (K), and flow velocity (m/s), respectively.

Poisson's equation represents that when an excess charge exists at an electrode surface, a potential changes abruptly. The modified NP equations describe time-dependent ion transport phenomena due to diffusion driven by concentration difference and migration driven by an electric field. In a salt removal phase, the salt ions move toward electrode surface and accumulate there by migration. Since ions accumulate at the electrode surface, excess charge appears and potential drops abruptly at that place by Poisson's equation leading to decrease in migration.

The PNP equations work well under less concentrated region; however, it is not applicable under highly concentrated region, i.e. electrode surface. The reasonable and efficient way to consider the highly concentrated region is to adopt a Stern layer:

$$\varphi_s + \lambda_s\nabla\varphi|_s = \varphi_{wall}, \quad (4)$$

where φ_s, λ_s,$\nabla\varphi|_s$, and φ_{wall} represent potential at Stern layer (V), effective Stern layer thickness (m), potential gradient at Stern layer (V/m), and potential at wall (V), respectively.

The effective Stern layer thickness (λ_s) in Eq. (4) represents the distance between the first layer of adsorbed ions and the wall. Equation 4 means that potential changes linearly inside Stern layer, or there is no excess ion between the first layer of adsorbed ions and the wall. By considering this Stern layer, the capacity of CDI electrodes can be predicted by PNP equations reasonably ($\sim$20 μF/cm^2).

Because the PNP equations cannot be solved theoretically, we computed them numerically. The computing procedure is given in Fig. 2. We solved the PNP equations simultaneously rather than sequentially. Because Poisson's equation and the modified NP equations are coupled tightly, sequential calculation becomes unstable and the computing load becomes too heavy. Therefore, for the first time, we solve the PNP equations simultaneously for the two-dimensional domain of CDI electrodes.

The simulation tool was verified, in our previous paper, for one-dimensional calculation by a theoretical model at an equilibrium case and by the other simulation code at a transient case [9]. The verification confirmed the well-construction of the simulation tool.

After the verification of the simulation tool, the tool was applied to a CDI facility. The two-dimensional domain for a CDI facility is given in Fig. 3. Since a CDI facility involves too many pores, we divided the CDI facility into several cells that contain one representative pore inside each cell. Total adsorption amount by a whole electrode is obtained by

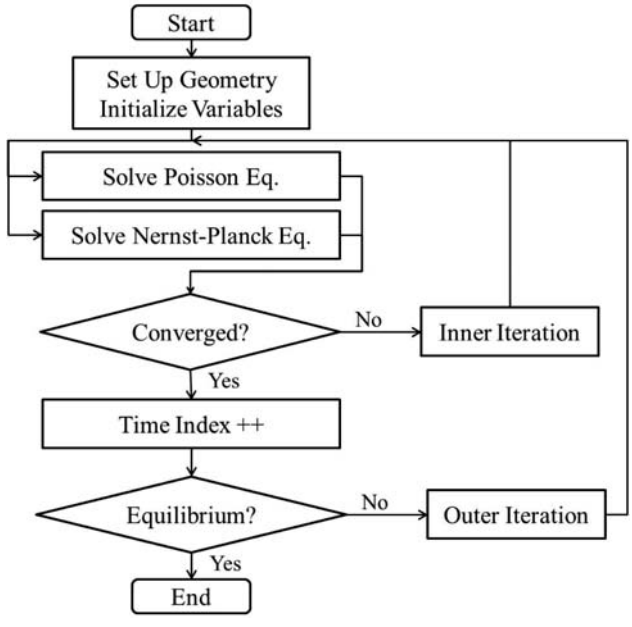

Fig. 2. Flowchart showing numerical computing process for a CDI electrode pore.

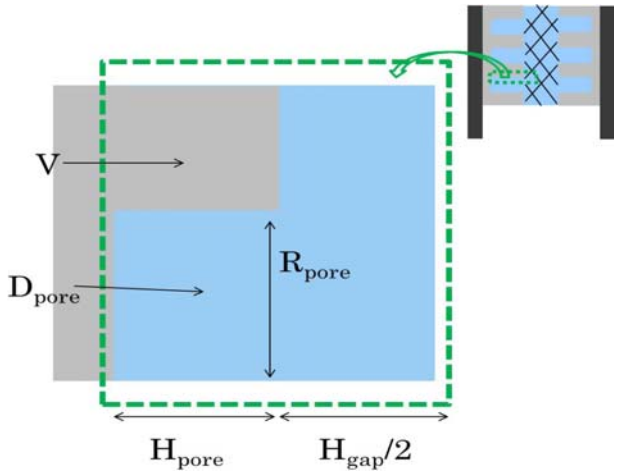

Fig. 3. System parameters in the simulation domain of a CDI electrode pore.

multiplication of adsorption amount of a pore by pore numbers. The representative pore is modeled to be cylindrical. The developed tool involves various parameters such as pore radius, pore depth, and pore diffusion coefficient. As a result, the tool is proper for optimization of electrode as well as for simulation of electrodes.

A sensitivity study was performed by varying system parameters in a CDI facility [9]. The key performance indicator (KPI) is defined as an inverse of capital cost of CDI facility. The operation cost of CDI facility is not considered because the value depends more on energy recovery than on electrode configuration. As a result, the following equation was obtained:

$$\mathrm{KPI} \propto (\sigma_{pore})^{1.0}(H_{pore})^{-0.7}(H_{gap})^{-0.3}(D_{pore})^{0.85}(R_{pore})^{-0.77}, \quad (5)$$

where σ_{pore}, H_{pore}, H_{gap}, D_{pore}, and R_{pore} represent the pore capacitance ($\mu F/cm^2$), pore depth (m), electrode gap distance (m), pore diffusion coefficient (m^2/s), and pore radius (m), respectively.

In Eq. (5), the capacitance, σ_{pore}, expresses salt removal amount of CDI electrodes. The value is reported to be a function of pore radius, R_{pore}. When the pore radius becomes smaller to be less than 1 nm, salt ions cannot enter the pore thereby lowering the capacitance. This is the very reason why mesoporous electrodes with larger pores have got attention. In this simulation tool, the capacitance decrease inside a sub-nanometer pore is not available to be predicted well theoretically. To account for a finite ion size inside smaller pores, a steric effect should be implemented in an efficient manner though adoption of the effect destabilizes the numerical calculation of the tool [11]. Furthermore, the capacitance, σ_{pore}, can be increased when the wettability of electrodes increases. Higher wettability eases the access of salt ions into the pores.

In Eq. (5), H_{pore} and H_{gap} are absolutely preferred to be small because distance for ions to transport becomes short, or the rate of adsorption becomes fast. Comparing the exponent numbers of H_{pore} and H_{gap}, -0.7 and -0.3, it becomes clear that the depth of pore is more important over the gap between electrodes. The difference comes from the sluggish movement of ions inside pores making the pore depth a bottle neck in the overall operating time of CDI.

In Eq. (5), D_{pore} is rarely measured for nanometer pores. The diffusion coefficient was measure to be in the order of 0.001 D_{bulk}, a diffusion coefficient in open area [12].

Eq. (5) is valid when the range of pore depth (H_{pore}), gap distance (H_{gap}), and pore diffusion coefficient (D_{pore}) are 200–800 μm, 100–400 μm, 0.001–0.1 D_{bulk}, respectively. The underlying assumption for Eq. (6) is that each parameter is independent and geometry of pores is cylindrical. These assumptions claim that the correlation of Eq. (5) is not exactly precise in exponent numbers but can give the overall trend of CDI performance in terms of system parameters. To make a precise correlation, experiments under various electrodes and system parameters should be performed.

Eq. (5) proves the importance of the capacitance, diffusion coefficient, pore radius, and pore depth on KPI. However, the capacitance and diffusion coefficient are not predictable theoretically. In the following sections, we will present methodology as well as results to measure the values for sample carbon aerogel electrodes.

3. Experimental methods for CDI evaluation

The experimental facility for CDI evaluation is given in Fig. 4. The carbon aerogel electrodes were purchased from Marketech. The electrode was cut into a 5 cm × 5 cm sheet; then a pair of sheets, one for cathode and the other for anode, were mounted in parallel onto a CDI facility. Between the electrode sheets, a piece of filter paper was placed to avoid short circuit. The gap between the electrodes is obtained to be 1.0 mm by measuring resistance of electrolyte and using the following equation: (gap in m) = (resistance in Ω) × (conductivity in $\Omega^{-1}\,m^{-1}$) × (electrode area in m^2). Saline water of 0.01 M NaCl was prepared as an influent. Nitrogen was purged onto the influent water to remove dissolved oxygen thereby suppressing chemical reactions [13]. The influent was injected into

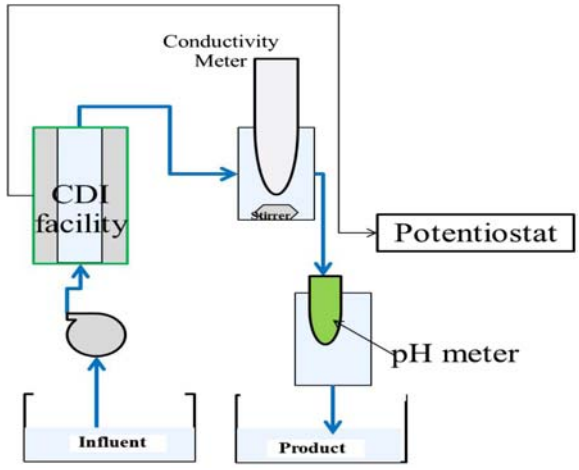

Fig. 4. Experimental cycle for CDI operation.

the CDI facility via a peristaltic pump at a flow rate of 27 mL/min. Using a potentiostat (Reference 600, Gamry Inst.), a constant potential was imposed across the electrodes; then, salt ions were adsorbed onto the surface of electrodes. To prevent a sudden soar of current, a potential increase rate was set to be 200 mV/s. The applied potential was maintained for 300 s; after that time, the potential was reduced to 0 V and maintained again for 300 s so that adsorbed ions are fully released into flushing water. This adsorption/desorption process in the CDI facility can be analyzed in two ways: decrease/increase in outlet conductivity and generation of current. The conductivity profile was measured by a conductivity meter for effluent water. The concentration and conductivity have a linear relation that one could be easily converted into the other. The current was measured by the potentiostat.

Four sets of experiments were performed with different applied potentials; 1.2, 1.0, 0.8, and 0.6 V. The current was integrated to give accumulated charge over a period of time. The accumulation of ions occurs at salt removal phase and dispersion of ions occurs at electrode recovery phase. The problem is that the charge does not go down to zero after the electrode recovery phase. The leakage charge comes from chemical reactions which will not totally disappear by nitrogen purging. For the purpose of analysis, which considers only physical adsorption, the leakage charge is subtracted under the assumption that the leakage current happens only under the salt removal phase at a constant rate.

The computing procedure for simulation of CDI operation with a carbon aerogel electrode is outlined in Fig. 5. The capacitance is obtained directly by interpreting current data; then, the developed simulation tool is applied for measurement of diffusion coefficient for CDI electrodes.

The average capacitance of a CDI electrode pore (σ_{avg}) is defined as an adsorption charge ($Q_{removal}$) at equilibrium divided by half an applied voltage ($\varphi/2$) and internal surface area ($A_{internal}$) as shown in Eq. (6).

$$\sigma_{avg} = \frac{Q_{charge}}{(\varphi/2)(A_{internal})} = \frac{\int Idt}{(\varphi/2)(A_{internal})}, \quad (6)$$

where σ_{avg}, Q_{charge}, I, φ, and $A_{internal}$ represent the average capacitance (F/m^2), charging amount (C), current that flows through CDI electrodes (A), applied voltage (V), and internal surface area of electrodes (m^2), respectively.

The diffusion coefficient of a CDI electrode pore (D_{pore}) is measured by the simulation tool. The simulation tool needs the capacitance, pore depth, pore radius for initial setting. The measured capacitance is entered by changing the effective Stern layer thickness inside the simulation tool. Although the pore depth is difficult to define due to its complex geometry, in this calculation, the pore shape is modeled to be straight cylindrical with its depth same as the electrode thickness, 0.254 mm. The average radius of the pores was obtained from the BJH method to be 5 nm and the internal area of electrodes ($A_{internal}$) is measured to be 99.17 m^2/cell from the BET result. The number of pores is calculated from Eq. (7):

$$N_{pore} = \frac{A_{internal}}{2\pi R_{pore} H_{pore}}, \quad (7)$$

where R_{pore}, H_{pore}, N_{pore}, and $A_{internal}$ represent the pore radius, pore depth, total pore number, and internal area of electrodes, respectively. Eq. (7) represents that the internal area of an electrode is the same as the surface area of the cylindrical pores and is established based on the cylindrical pore model with a uniform pore radius and depth. From Eq. (7), N_{pore} is estimated to be 1.24×10^{13}. The pore diffusion coef-

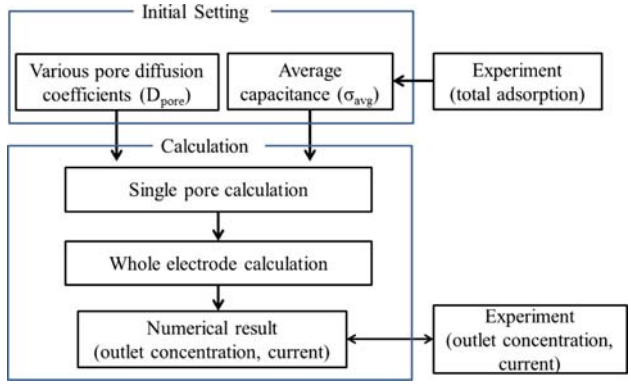

Fig. 5. Computing procedure for the simulation of CDI operation with a carbon aerogel electrode.

ficient is varied to determine the appropriate value by comparing the simulation results with the experiment results. After the initial setting, numerical calculation was conducted. The simulation tool that deals with a single pore was extended into the one that covers the entire surface of an electrode. Since manipulation inside all pores requires too much computational power, the electrode is divided into several computational cells where each cell contains one representative pore.

4. Results and discussion

The accumulated charge profiles from different applied potentials are given in Fig. 6. The profile involves both adsorption or desorption of salt ions and unwanted chemical reactions. By subtracting the chemical reaction, we can obtain only charges that come from adsorption or desorption of salt ions as shown in Fig. 7. This charge profile was used to measure the capacitances and diffusion coefficients of electrodes. The capacitances were calculated from Eq. (6). To obtain the diffusion coefficients, the conditions for these experiments, which are given in Table 1, were entered into the initial setting of the developed simulation code. The charge profiles were fitted by the simulation tool and the results are given in the same figure, Fig. 7. For each potential, the calculated capacitance and diffusion coefficients are given in Table 2. Capacitance decreases mildly as potential decreases. Doubling the potential from 0.6 to 1.2 V makes a 25% increase in the capacitance value. It means that we should apply as high potential as possible within the window of suppressing chemical reactions. Diffusion coefficients inside pores are expressed in terms of the diffusion

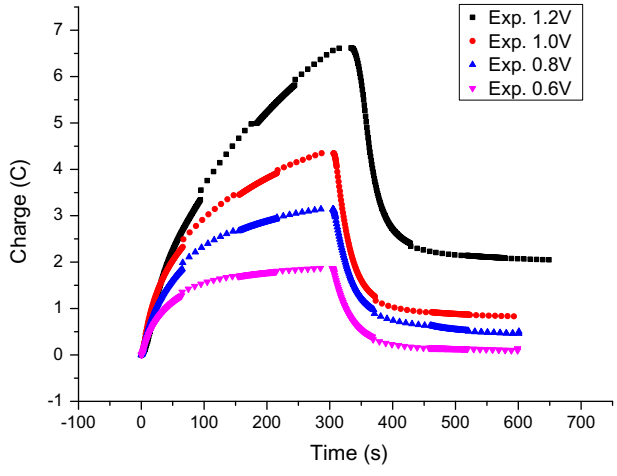

Fig. 6. Accumulated charge profile of carbon aerogel electrode at various applied potentials (without modification).

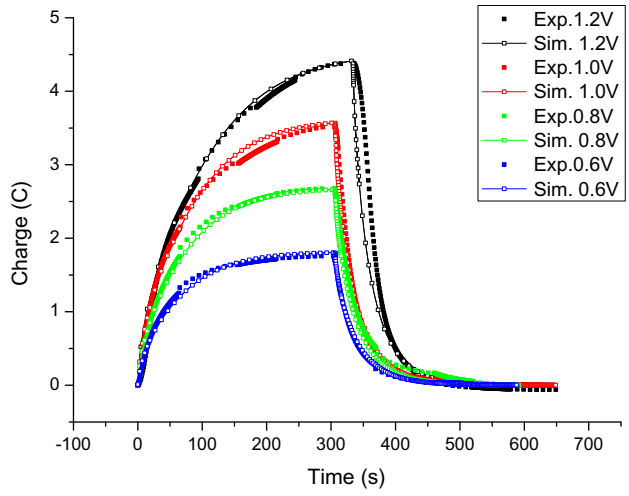

Fig. 7. Modified charge profile (subtracted chemical reaction current) of carbon aerogel electrodes and simulation results for the profile (capacitance and diffusion coefficients are given in Table 2).

coefficient in bulk water. The coefficients inside pores are smaller than the one in bulk water because of two reasons: sluggish movement of ions inside narrow pores and repulsive force among ions. This phenomenon of low diffusion coefficients inside small pores is already reported [12]. Regarding the first reason, since sodium and chloride ions with the hydrated ion radii of around 0.35 nm are restricted inside few nanometer pores, the ions collide with the wall of pores to lose their momentum. Regarding the second reason, since ions accumulate inside pores, the distance between ions becomes too small to be neglected. For example, for the applied potential of 1.2 V, the average distance between co-ions is estimated to be 15 nm by the simulation code, which calculates the distance by the following equation: $d = c_{\max}^{-1/3}$. Considering the fact that the ion distances of 0.01 M NaCl in bulk water and in closely packed arrangement are 55 nm (both co-ions and counter-ions) and 0.7 nm (twice the hydrated radii), respectively, the distance among co-ions is shortened. These two reasons retard the movement of ions at the first phase. However, in the second phase, the repulsive force aids ion release thereby increasing the diffusion coefficient. That is the reason why the diffusion coefficient at the salt removal phase is smaller than the one at the electrode recovery phase. Because of the first reason, the narrow pore reduces the coefficients by 100 times, whereas, because of the second reason, repulsive force decreases (at first phase) or increases (at second phase) them by 3–6 times. The diffusion coefficients increase gradually as potential decreases because of the decreased concentration of ions inside pores, for example, 487 mM at 1.2 V to 110 mM at 0.6 V.

Table 1
Design parameters for the carbon aerogel electrode experiment

Parameters	Values
Influent concentration	0.01 M (~1,400 μS/cm)
Flow rate	27 mL/min
Electrode type	Carbon aerogel electrode
Gap distance	1 mm
Electrode dimension	5 cm × 5 cm × 0.0254 cm (Mass: 0.4 g)

Table 2
Capacitance and pore diffusion coefficients calculated from the simulation tool

Potential (V)	Capacitance (μF/cm^2)	Diffusion coefficient (1st phase)	Diffusion coefficient (2nd phase)
1.2	7.4	0.01 D_{bulk}	0.06 D_{bulk}
1.0	7.1	0.015 D_{bulk}	0.06 D_{bulk}
0.8	6.7	0.02 D_{bulk}	0.06 D_{bulk}
0.6	5.9	0.025 D_{bulk}	0.06 D_{bulk}

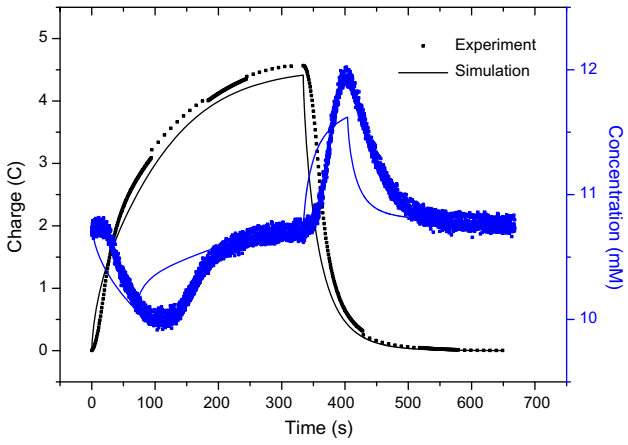

Fig. 8. Accumulated charge profile and the outlet concentration for a carbon aerogel electrode under 1.2 V.

For further validation of the capacitance and diffusion coefficient values, we compared the outlet concentration profile obtained through the experiment and the simulation under 1.2 V. Due to chemical reactions occurred during the salt removal phase, the desorption amount was measured to be higher than the adsorption amount by around 2 C, which is similar to the leakage charge noticed in the current measurement. That mismatch is solved by increasing the adsorption amount to the level of desorption amount. The comparison in both the accumulated charge and the outlet concentration between the simulation and the experiment is displayed in Fig. 8. Though the overall trend was simulated successfully, the total amount of salt removed and detailed profile were different. The differences can come from insufficient understanding of current leakage and residence of saline water inside a glass with the conductivity meter. Regarding the first aspect, there have been no general explanations about the chemical reactions though some trials were made. Simple subtraction or addition of current and salt adsorption might not exclude current leakage perfectly. Better understanding or ruling out of chemical reactions can aid future simulation and understanding of CDI operation. Regarding the second aspect, since the effluent water out of the CDI test section resides inside the measurement chamber of the concentration for a while, the outlet concentration measured from the experiment shows the mild change whereas the one from the simulation shows the steep change after reaching its minimum/maximum values.

5. Conclusions

We developed a simulation tool which reflects characteristics of electrodes solving the Poisson–Nernst–Planck equation using a coupled numerical scheme. The simulation tool enables us to obtain the most effective design parameters of CDI electrodes: pore depth, pore radius, capacitance, and pore diffusion coefficient. The calculation results of the capacitance and diffusion coefficients of a carbon aerogel electrode are around 7.5 μF/cm^2 and 0.01 D_{bulk}, respectively. Also, we found out that the diffusion coefficient at the electrode recovery phase is by 3–6 times higher than that at the salt removal phase. The diffusion coefficients increase gradually as potential decreases because of the decreased concentration of ions inside pores. The low diffusion coefficient is reasoned to come from the existence of narrow pores and repulsion between co-ions. While most of previous

research activities mainly focused on capacitance, the current research highlights the importance of diffusion coefficients, which determines the required amount of electrodes. The electrode assessment was performed for carbon aerogel electrodes only; however, in the future, various electrodes are required to be analyzed for comparison and optimization.

Acknowledgments

The authors gratefully acknowledge that this was undertaken for 'Conceptual Design and Experimental Validation of Core Technologies for WHEN (Water-Hydrogen-Electricity-Nuclear reactor) System' and financially supported by the Korean Ministry of Education, Science and Technology.

Nomenclature

T	—	time, s
C	—	concentration, mol/m^3
D_{pore}	—	pore diffusion coefficient, m^2/s
D_{bulk}	—	bulk diffusion coefficient, m^2/s
F	—	Faraday constant, C/mol
H_{pore}	—	pore depth, m
H_{gap}	—	gap distance between electrodes, m
Q_{charge}	—	charging amount, C
R_{pore}	—	pore radius, m
U	—	flow velocity, m/s
φ	—	potential, applied potential, V
ρ	—	excess charge, C/m^3
ε	—	permittivity, F/m
λ_s	—	stern layer thickness, m
φ	—	applied voltage, V
σ	—	capacitance, F/m^2

Subscripts

s	—	Stern layer
wall	—	wall
pore	—	pore properties
avg	—	average

References

[1] I.C. Karagiannis, P.G. Soldatos, Water desalination cost literature: review and assessment, Desalination 223 (2008) 448–456.
[2] T.J. Welgemoed, C.F. Schutte, Capacitive Deionization Technology^{TM}: An alternative desalination solution, Desalination 183 (2005) 327–340.
[3] J.C. Farmer, D.V. Fix, G.V. Mack, R.W. Pekala, J.F. Poco, Capacitive deionization of NaCl and $NaNO_3$ solutions with carbon aerogel electrodes, J. Electrochem. Soc. 143(1) (1996) 159–169.
[4] J.B. Lee, K.K. Park, S.W. Yoon, P.Y. Park, K.I. Park, C.W. Lee, Desalination performance of a carbon-based composite electrode, Desalination 237 (2009) 155–161.
[5] L. Zou, L. Li, H. Song, G. Morris, Using mesoporous carbon electrodes for brackish water desalination, Water Res. 42 (2008) 2340–2348.
[6] S. Nadakatti, M. Tendulkar, M. Kadam, Use of mesoporous conductive carbon black to enhance performance of activated carbon electrodes in capacitive deionization technology, Desalination 268 (2010) 182–188.
[7] J.S. Kim, J.H. Choi, Fabrication and characterization of a carbon electrode coated with cation-exchange polymer for the membrane capacitive deionization applications, J. Membr. Sci. 335 (2010) 85–90.
[8] P.M. Biesheuvel, B. van Limpt, A. van der Wal, Dynamics adsorption/desorption process model for capacitive deionization, J. Phys. Chem. C 113 (2009) 5636–5640.
[9] B.G. Jeon, H.C. NO, J.I. Lee, Development of a two-dimensional coupled-implicit numerical tool for the optimal design of CDI electrodes, Desalination 274 (2011) 226–236.
[10] B.G. Jeon, H.C. NO, J.I. Lee, Development of a two-dimensional coupled-implicit numerical tool for analysis of the CDI operation, Desalination 288 (2012) 66–71.
[11] M.S. Kilic, M.Z. Bazant, Steric effects in the dynamics of electrolytes at large applied voltages. 1. Double-layer charging, Phys. Rev. E 75 (2007) 021502.
[12] H. Malmberg, M. Zuleta, A. Lundblad, P. Bjornbom, Ion transport in pores in activated carbons for EDLCs, J. Electrochem. Soc. 153(10) (2006) A1914–A1921.
[13] Y. Bouhadana, M. Ben-Tzion, A. Soffer, D. Aurbach, A control system for operating and investigating reactors: the demonstration of parasitic reactions in the water desalination by capacitive de-ionization, Desalination 268 (2011) 253–261.